An Optimized Procedure for Metabonomic Analysis of Rat Liver Tissue Using Gas Chromatography/Time-of-Flight Mass Spectrometry

By: Li Pan, Yunping Qiu, Tianlu Chen, Jinchao Lin, Yi Chi, Mingming Su, Aihua Zhao, and Wei Jia

Pan, L., Qiu, Y., Chen, T., Lin, J., Chi, Y., Su, M., Zhao, A., Jia, W. (2010). An optimized procedure for metabonomic analysis of rat liver tissue using gas chromatography/time-of-flight mass spectrometry. *Journal of Pharmaceutical and Biomedical Analysis, 52,* 589–596.

Abstract:

In this paper, we present a tissue metabonomic method with an optimized extraction procedure followed by instrumental analysis with gas chromatography/time-of-flight mass spectrometry (GC/TOFMS) and spectral data analysis with multivariate statistics. Metabolite extractions were carried out using three solvents: chloroform, methanol, and water, with design of experiment (DOE) theory and multivariate statistical analysis. A two-step metabolite extraction procedure was optimized using a mixed solvent of chloroform–methanol–water (1:2:1, v/v/v) and then followed by methanol alone. This approach was subsequently validated using standard compounds and liver tissues. Calibration curves were obtained in the range of 0.50–125.0 μg/mL for standards and 0.02–0.25 g/mL acceptable for liver tissue samples. For most of the metabolites investigated, relative standard deviations (RSD) were below 10% within a day (reproducibility) and below 15% within a week (stability). Rat liver tissues of carbon tetrachloride-induced acute liver injury models (n = 10) and healthy control rats (n = 10) were analyzed which demonstrated the applicability of the developed procedure for the tissue metabonomic study.

Article:

INTRODUCTION

As end products of biochemical regulations and metabolism, metabolites represent the response to the genomic and environmental action of cells. The measurement of metabolome variations in response to stimuli has been widely used in modern pharmaceutical and biomedical research [1,2]. The main analytical methods employed for metabonomic studies are based on information-rich spectroscopic techniques, such as nuclear magnetic resonance (NMR) spectrometry and mass spectrometry (MS), which is usually coupled with gas chromatography (GC/MS), liquid chromatography (LC/MS) or capillary electrophoresis (CE/MS) [3-5]. Metabonomic studies generate complex multivariate data that requires chemometrics for interpretation [6]. With unsupervised methods like principle components analysis (PCA) [7], and supervised methods

such as partial least square (PLS) [8] and orthogonal partial least square (OPLS) analysis [9], researchers can obtain classification patterns and identify the compounds responsible for such patterns and grouping.

Biofluids such as urine and blood are most frequently used in metabonomic studies, because they contain a wide variety of metabolites and can be obtained non-invasively. However, urine and blood metabonomics reflect the comprehensive metabolic effects associated with a pathogen or chemical agent stimuli; they are unable to provide the precise perspective of local metabolism and microenvironment [10]. Therefore, tissue-targeted technology has considerable value since many diseases may cause detectable disturbances only to the local metabolic pathways within specific organs [11]. Tissue-targeted metabonomic analyses have been carried out on brain tissue [11-13], liver tissue [14-16], and kidney tissue [17-19]. Metabolite extraction is a critical step in tissue metabonomic study, and the chloroform–methanol–water solvent system is considered the preferred method in several reports [20-23]. The latest relevant study was conducted by Wu et al. [24], in which fish liver was used to optimize the extraction strategy of the preferred solvent system for NMR- and FT-ICR MS-based metabonomic studies. However, the optimized ratio of solvent mixture and extraction method used specifically for GC/MS-based tissue metabonomics has not yet been determined.

In this study, we combined design of experiment (DOE) theory [25] with multivariate statistical analysis to optimize the ratio of solvents in the preferred extraction system chloroform–methanol–water and the method for maximum extraction of metabolites from rat liver tissue, using gas chromatography/time-of-flight mass spectrometry (GC/TOFMS). The methodology was then validated by method validations using standard compounds and liver tissues from healthy rats. The established procedure was then utilized to discriminate carbon tetrachloride (CCl_4)-induced acute liver injury rats from healthy controls and to detect the metabolite variations in the liver tissues.

MATERIALS AND METHODS

Chemicals and reagents

Ultrapure water from the Milli-Q system (Millipore, USA) was used in the experiments. Chromatographic grade methanol was purchased from Merck Chemicals (Germany). Chloroform, aether, olive oil, CCl_4, pyridine, and anhydrous sodium sulfate were analytical grade and purchased from China National Pharmaceutical Group Corporation (Shanghai, China). l-2-chlorophenylalanine (Intechem Tech. Co., Ltd., Shanghai, China) and heptadecanoic acid (Sigma–Aldrich, St. Louis, MO, USA) served as internal standards. BSTFA (1% TMCS), methoxyamine, and the 29 standard compounds (Table 2) were purchased from Sigma–Aldrich (St. Louis, MO, USA) and properly stored before use. Superoxide dismutase (SOD) testing kits and malondialdehyde (MDA) testing kits were purchased from the Jiancheng Institute of Biotechnology (Nanjing, China).

Animal handling and sampling

Twenty male Sprague–Dawley rats weighing 220 ± 20 g were purchased from Shanghai Laboratory Animal Co., Ltd. (SLAC, Shanghai, China). The rats were maintained in a 12-h light/12-h dark cycle at 25 °C and 50% humidity, with free access to food and water. After a week acclimation, the rats were randomly divided into two groups: liver injury model group

(n = 10) and control group (n = 10). The model rats received intra-peritoneal injections twice (24 h interval) with a dose of 1.5 mL/kg (body weight) CCl_4 solution (diluted twofold with olive oil) to induce acute liver injury. The control rats received an equal volume of olive oil by intra-peritoneal injections. All rats were sacrificed 24 h after the second injection, after collecting blood from the heart under aether anesthesia. The collected blood was clotted at room temperature and the serum was separated by centrifugation. Rat livers were removed from the body immediately after sacrifice and washed in ice-cold physical saline solution. The isolated livers and serum were stored at −80 °C until use. Liver tissues used in the following extraction investigations were chosen randomly from rats in the healthy control group.

Extraction method

One-step extraction. We investigated the ability of various ratios of the three solvents in the preferred solvent system – chloroform, methanol, and water – to extract metabolites from liver tissue. A total of 1000 µL solvent was used for each 100 mg of liver tissue. The volumes of chloroform and water were both limited to 250 µL of the total 1000-µL mixture (discussed below) and ten different solvent mixtures were obtained from a D-optional experimental design using MODDE software (Umetrics, Umeå, Sweden) (Table 1). Each experiment was performed twice to test its repeatability. The following process was used for metabolite extraction: liver tissues were weighed and homogenized with a T10 basic homogenizer (IKA, Staufen, Germany) for 30 s at 0 °C, then centrifuged at 12,000 rpm for 10 min at 4 °C. The resulting supernatant (300 µL) was transferred to a GC sampling vial containing two internal standards, l-2-chlorophenylalanine (10 µL, 0.3 mg/mL) and heptadecanoic acid (10 µL, 1.0 mg/mL), then dried in a vacuum centrifuge concentrator before the subsequent derivatization.

Table 1: Solvent mixtures tested in one-step extraction.

No.[a]	Chloroform	Methanol	Water	v/v/v[b]
01	0 µL	1000 µL	0 µL	0:1:0
02	0 µL	750 µL	250 µL	0:3:1
03	250 µL	500 µL	250 µL	1:2:1
04	250 µL	750 µL	0 µL	1:3:0
05	125 µL	875 µL	0 µL	1:7:0
06	0 µL	875 µL	125 µL	0:7:1
07	125 µL	750 µL	125 µL	1:6:1
08	125 µL	625 µL	250 µL	1:5:2
09	200 µL	600 µL	200 µL	1:3:1
10	220 µL	560 µL	220 µL	2:5:2

[a]Each experiment has one replicate.
[b]Chloroform:methanol:water, v/v/v.

Two-step extraction. Based on the results of one-step extraction, a two-step extraction procedure was carried out. For each 100-mg liver tissue sample, 500 µL of each of the two solvents (the mixture of chloroform, methanol and water (1:2:1, v/v/v); and methanol alone) were used to determine the optimal order of the two extraction solvents. After homogenization with the first solvent and centrifugation, a 150-µL aliquot of supernatant was transferred to a GC sampling vial containing the internal standards and the deposit was re-homogenized with the second solvent before a second centrifugation. Another 150-µL aliquot of supernatant was added to the same vial for drying and then derivatization as described below.

Method validation

Linearity. The linearity of standards was determined by mixing 29 standard compounds (see Table 2) belonging to different chemical classes – amino acids, organic acids, carbohydrates,

fatty acids, nucleotides – and diluted to concentrations of 0.004, 0.020, 0.050, 0.100, 0.200, 0.400 and 1.000 of their original concentrations, ranging from 0.5 to 125 μg/mL or 1.0 to 250 μg/mL. Each 100 μL mixture solution was added to the sampling vial with two internal standards, l-2-chlorophenylalanine (10 μL, 0.3 mg/mL) and heptadecanoic acid (10 μL, 1.0 mg/mL), and then dried in a vacuum centrifuge concentrator before subsequent derivatization.

Table 2: Linearity and detection limit of mixed standards and liver tissue samples.

Compounds investigated	Linear range of mixed standards (μg/mL)[a]	*n*	r^{2b}	Linear range of tissue samples (g/mL)	*n*	r^{2b}	Detection limit	
							pg on column[c]	S/N ratio[d]
Amino acids								
Tyrosine	0.50–125.0	7	0.999	0.02–0.25	7	0.994	125.0	34.4
Tryptophan	0.50–125.0	7	0.992	0.02–0.25	7	0.999	312.5	55.9
Glycine	0.50–125.0	7	0.999	0.02–0.25	7	0.989	15.6	46.8
Proline	0.50–125.0	7	0.996	0.02–0.25	7	0.996	15.6	56.9
Aspartic acid	0.50–125.0	7	0.997	0.02–0.25	7	0.991	31.3	35.7
Methionine	0.50–125.0	7	0.998	0.02–0.25	7	0.994	62.5	49.5
Valine	0.50–125.0	7	0.998	0.02–0.25	7	0.997	15.6	47.2
Alanine	0.50–125.0	7	0.997	0.02–0.25	7	0.987	15.6	80.9
Serine	0.50–125.0	7	0.997	0.02–0.25	7	0.995	15.6	23.9
Isoleucine	0.50–125.0	7	0.997	0.02–0.25	7	0.996	31.3	10.9
Histidine	1.00–250.0	7	0.988	0.02–0.25	7	0.997	312.5	66.4
Threonine	0.50–125.0	7	0.993	0.02–0.25	7	0.996	31.3	15.5
Asparagine	0.50–125.0	7	0.999	0.02–0.25	7	0.996	31.3	4.8
Ornithine	1.00–250.0	7	0.999	0.02–0.25	7	0.993	62.5	44.7
Lysine	0.50–125.0	7	0.996	0.02–0.25	7	0.995	156.3	58.4
4-Aminobutyric acid	0.50–125.0	7	0.995	0.02–0.25	7	0.983	31.3	46.9
Organic acids								
Citric acid	0.50–125.0	7	0.992	0.02–0.25	7	0.985	312.5	56.7
Succinic acid	0.50–125.0	7	0.996	0.02–0.25	7	0.993	15.6	49.1
α-Ketoglutaric acid	1.00–250.0	7	0.997	0.02–0.25	7	0.989	625.0	20.5
Carbohydrates								
Fructose	0.50–125.0	7	0.998	0.02–0.15	6	0.989	156.3	42.9
Arabitol	1.00–250.0	7	0.999	0.02–0.25	7	0.985	125.0	65.2
Gluconic acid	0.50–125.0	7	0.999	0.02–0.25	7	0.999	1562.5	99.9
Fatty acids								
Tetradecanoic acid	1.00–250.0	7	0.996	0.05–0.25	6	0.999	31.3	35.2
Hexadecanoic acid	1.00–250.0	7	0.999	0.02–0.25	7	0.986	15.6	109.8
Oleic acid	1.00–250.0	7	0.997	0.02–0.25	7	0.983	125.0	32.4
Octadecanoic acid	1.00–250.0	7	0.994	0.02–0.25	7	0.990	15.6	91.5
Nucleotides								
Thymine	2.50–125.0	6	0.999	0.02–0.25	7	0.980	15.6	29.8
Adenosine	2.50–125.0	6	0.997	0.05–0.25	6	0.977	625.0	14.8
Uridine	1.00–250.0	7	0.998	0.02–0.15	6	0.990	1562.5	38.9

[a]Standard compounds (stored at −4 °C before use) were diluted with water or methanol (for fatty acids).
[b]Correlation coefficients were calculated for the linear range listed in the table.
[c]Detection limit (pg on column) is the lowest calibration standard injected with a S/N ratio ≥3.
[d]S/N ratio was obtained using peak-to-peak values by ChromaTOF software.

The linearity of liver tissue samples was also investigated. A series of 20, 50, 75, 100, 125, 150 and 250 mg liver tissue samples were used in metabolite extraction by 500 μL solvent mixture of chloroform, methanol, and water (1:2:1, v/v/v) as the first step and another 500 μL methanol alone as the second step. Extracts were then dried and derivatized as described below.

The correlation coefficients (r^2) were calculated by the ratio of the peak area of each compound to the peak area of the corresponding internal standard in the analyzed concentration interval: l-2-chlorophenylalanine was used when the retention time of the standard's peak was less than 20 min and heptadecanoic acid used when the retention time was greater than 20 min.

Limit of detection. To determine the limit of detection for each standard compound, a mixed standard solution was further diluted to concentrations of 0.0002, 0.0004, 0.0008 and 0.002 of their original concentrations, ranging from 25 to 250 pg/mL or 50 to 500 pg/mL. Each 100 μL mixture solution was added to the sampling vial with two internal standards and then dried in a vacuum centrifuge concentrator before subsequent derivatization. The signal-to-noise ratio was calculated in the data analysis interface of the Leco ChromaTOF software (v3.30).

Precision, reproducibility, stability, and recovery. The instrument precision was obtained by continuously injecting the same sample vial of one mixed standard (12.5 or 25.0 μg/mL) six times and calculating the relative standard deviation (RSD) of the peak areas of standard compounds to the corresponding internal standard. The method reproducibility and stability were investigated using healthy rat liver tissue. Reproducibility was analyzed by repeating the whole method for the same liver tissue within a day (n = 6). Meanwhile, the stability test was performed by analyzing eight prepared samples from the same liver tissue on every other day within 1 week (ie, Days 1, 3, 5, 7; n = 2 for each day). The recovery of typical test metabolites was examined by adding mixed standards at three different concentrations (12.5, 25.0 and 50.0 μg/mL, or 25.0, 50.0 and 100.0 μg/mL; n = 3 for each concentration) to 50 mg liver tissue samples.

Derivatization procedure and GC/TOFMS analysis

The derivatization procedure was conducted with minor modifications to the previous serum metabonomic study report [25]. Briefly, 80-μL methoxyamine (15 mg/mL in pyridine) was added to dry sample vials and vortexed for 30 s. Methoxymation was carried out at 30 °C for 1.5 h. After adding another 80 μL BSTFA (containing 1% TMCS) and vortexing for 30 s, silylation was carried out at 70 °C for 1 h. Each 1-μL derivatized sample was injected into an Agilent 6890N gas chromatograph in splitless mode with time-of-flight mass spectrometry (Pegasus HT, Leco Co., CA, USA). Separation was achieved on a DB-5ms capillary column (30 m × 250 μm i.d., 0.25-μm film thickness; Agilent J&W Scientific, Folsom, CA, USA) using helium as the carrier gas, at a constant flow rate of 1.0 mL/min. The injector temperature was set at 270 °C. The GC oven temperature was set at 80 °C for the first 2 min, then programmed to ramp up 10 °C/min to 180 °C, 5 °C/min to 240 °C, 25 °C/min to 290 °C, and finally maintained at 290 °C for 9 min. Transfer line temperature and ion source temperature were set at 260 °C and 200 °C, respectively. The mass spectra were obtained with electron impact ionization (70 eV) at full scan mode (m/z 30–600).

Analysis of GC/TOFMS data

All GC/TOFMS files were analyzed and converted to CDF format by ChromaTOF software (v3.30, Leco Co., CA, USA). CDF files were extracted using custom scripts (revised Matlab toolbox HDA, developed by Jonsson et al. [26,27]) in the MATLAB 7.0 (The MathWorks, Inc., USA) for data pretreatment procedures such as baseline correction, de-noising, smoothing and alignment, time-window splitting, and peak feature extraction (based on multivariate curve

resolution algorithm) [27]. The resulting output data organized as arbitrary peak index (retention time-m/z pairs), sample names (observations), and peak intensity information (variables) were introduced into Simca-P 11.5 software (Umetrics, Umeå, Sweden) for principal components analysis (PCA), partial least squares (PLS) regression [28] and orthogonal partial least squares project to latent structures-discriminant analysis (OPLS-DA) [29]. Differential metabolites between model rat liver tissues and the controls generated from OPLS-DA model were identified by ChromaTOF software coupled with commercially available NIST library 2005 and some reference compounds.

RESULTS AND DISCUSSION

Extraction optimization

The percentages of water and chloroform in the solvent mixture were both limited to 25% in our extraction procedure. This limitation was based on the results of our pre-experiments. When the percentage of water or chloroform increased, some compounds, especially carbohydrates such as glucose, lactose, and maltose, produced multiple peaks with high intensity and broadened peaks (data not shown). This would not only cause difficulty in quantifying these metabolites, but also mask adjacent peaks generated by other metabolites. In addition, excess amount of water in the extraction process would lead to precipitation in the samples after derivatization, putting gas chromatograph at risk of contamination; while too much of chloroform would cause the separation between organic and aqueous layers during extraction.

A two-component PLS model [25,28] was generated to demonstrate the relationship between the **X** matrix (ie, the resolved peak areas of the metabolites of the 20 experimental samples in Table 1; each peak area is one *X*-variable) and the design matrix **Y** (ie, the ratios of the solvent mixtures tested in Table 1; the amounts of the three solvent involved in the mixture are three *Y* variables). The two-component PLS scores plot (R^2X = 0.602, R^2Y = 0.943, Q^2Y = 0.751) and the loading plots are shown in Fig. 1a and b. The first component explains 31.5% of the variance in the resolved peak areas, and the second component explains 28.7% of the variance. The PLS scores plot (t_1–t_2; Fig. 1a) shows how the areas of resolved peaks (X variables) correlate to the solvent compositions (shown as experiment number according to Table 1), and determine the distribution of experimental samples on the scores plot. For example, samples extracted with a mixture of chloroform, methanol, and water (Test Nos. 03, 07, 08, 09, 10; Table 1) are grouped together in the upper right quadrant of the plot; samples extracted with chloroform and methanol mixtures (Test Nos. 04 and 05) grouped in the upper left quadrant; samples with methanol alone (Test No. 01) located separately at the lower left quadrant.

Figure 1: (a) The PLS scores t_1 and t_2 of the experimental samples.

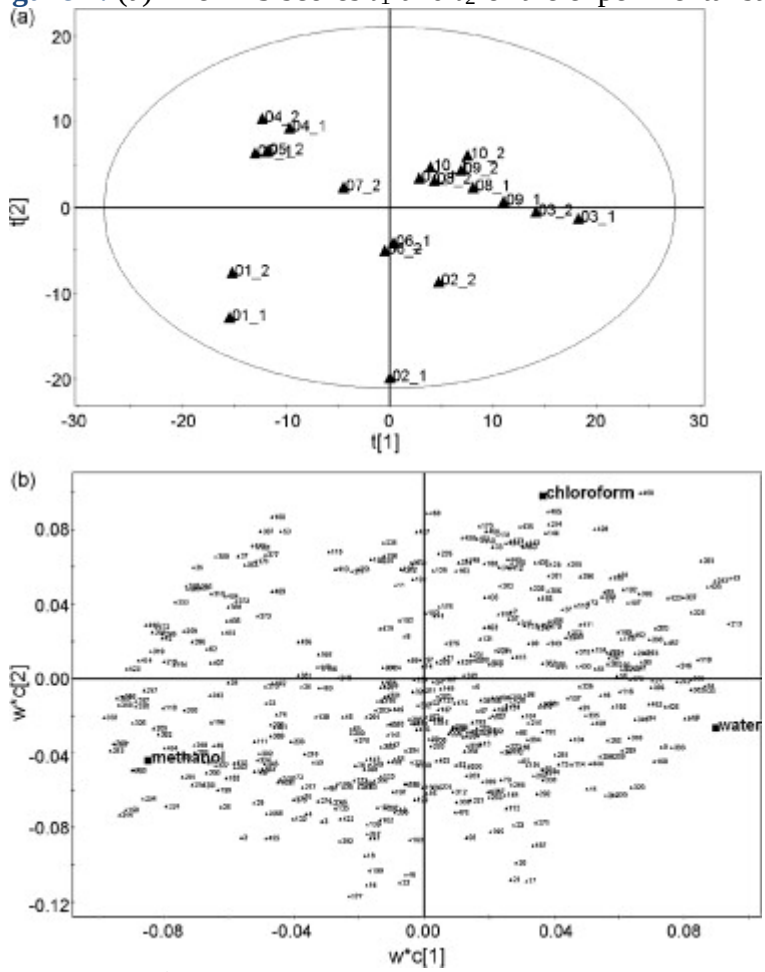

Each triangle stands for one designed experiment numbers in Table 1. (b) The PLS weights, *w** (*X*-weights) and *c* (*Y*-weights), for *X* variables (the areas of the resolved GC/TOFMS peaks) and *Y* variables (designed proportion of the three solvent), respectively.

The PLS loading plot (Fig. 1b, *w***c*-plot) summarizes the influence and correlation structure between variables in both the **X** matrix and the **Y** matrix. *X* variables with large *w**'s (*X*-weights, positive or negative; situated far away from the origin in the *w***c* loading plot) are highly correlated with *Y*; while *Y* variables with large *c*'s (*Y*-weights) are highly correlated with *X*. The *w***c* loading plot shows both the *X*-weights (*w**) and the *Y*-weights (*c*), and thereby reveals how the *X* and *Y* variables combine in the projections, and how the *X* variables relate to the *Y* variables. From Fig. 1b, we can see that the first PLS component is mainly dominated by water (positively) and methanol (negatively), and the second component mainly by chloroform (positively) and methanol (negatively). Peak areas (*X* variables) near the center of the loading plot are less affected by the compositions of the solvent mixture, while peaks far from the center are greatly affected by solvents (*Y* variables), either positively or negatively. The wide distribution of peak areas in the loading plot implies the necessity of a two-step extraction with each step having a different ratio of solvent mixture for the extraction of these metabolites in liver tissue. Due to the opposing effect of methanol and water (chloroform) on most peak areas, experimental No. 01 (containing methanol alone) and experimental No. 03 (chloroform:methanol:water = 1:2:1, v/v/v) were selected for each step of a two-step extraction, to maximize the number of metabolites effectively extracted for metabonomic analysis.

Apart from PLS modeling analysis, we can observe the complementary extraction ability of solvent mixture 03 (chloroform:methanol:water = 1:2:1, v/v/v) and 01 (methanol alone) from Fig. 2a and b. By comparison, methanol alone (Fig. 2b) produced more intense peaks for lipophilic compounds (eg, hexadecanoic acid, oleic acid, octadecanoic acid, uridine, and cholesterol); while the peak intensities of hydrophilic compounds (eg, serine, threonine, proline, glutamine, and phosphoric acid) seem to abate gradually.

Figure 2: Typical GC/TOFMS total ion current (TIC) chromatograms of liver tissue extracts using (a) one-step extraction (chloroform:methanol:water = 1:2:1, v/v/v), (b) one-step extraction (methanol alone), and (c) two-step extraction (first, chloroform:methanol:water = 1:2:1, v/v/v; second, methanol alone).

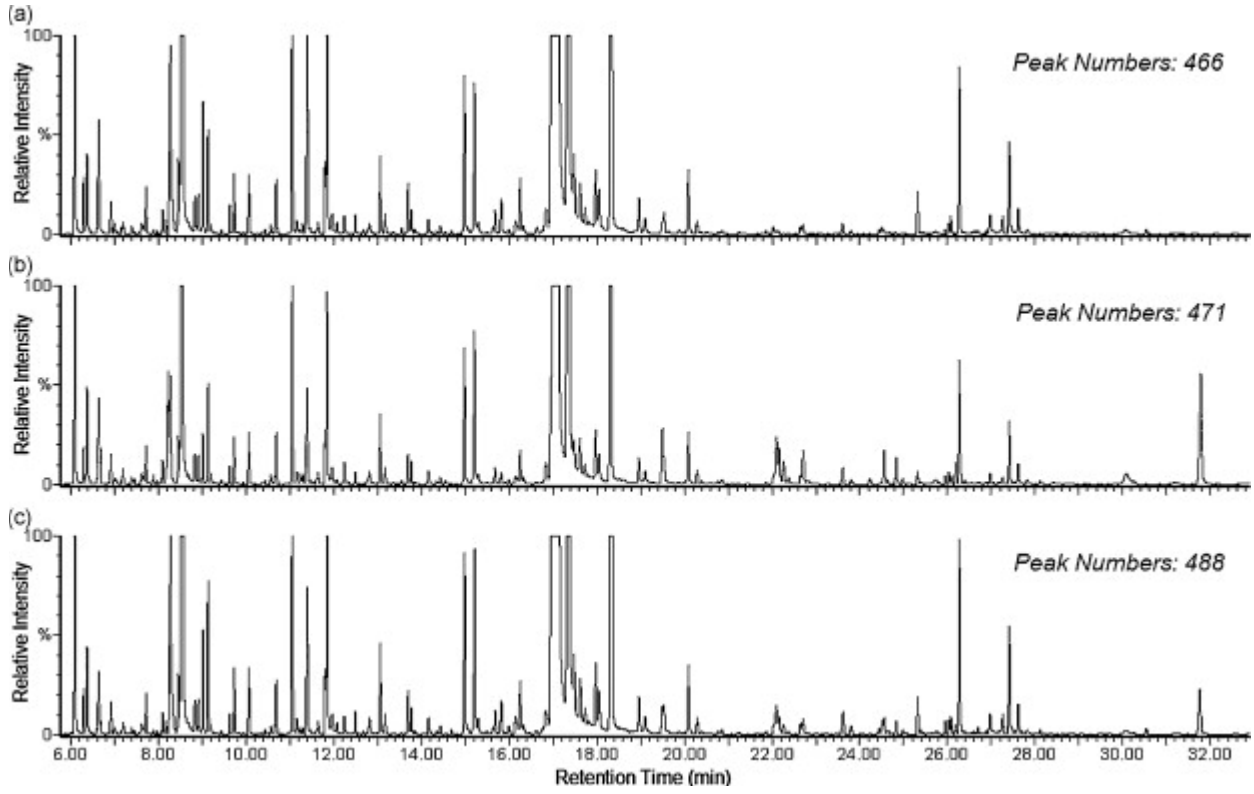

The sequence of the two solvents chosen for the two-step procedure was also investigated to optimize the extraction procedure. The results suggest that the solvent mixture (chloroform:methanol:water = 1:2:1, v/v/v) should be used prior to methanol alone. This may be necessary because the solvent mixture removes water from the liver tissue, allowing methanol alone in the second step to extract more lipophilic metabolites. The two-step method (Fig. 2c) seems to be an acceptable compromise between the specialized extractions required by hydrophilic and lipophilic metabolites from liver tissue in one-step extractions, with more GC/TOFMS peaks resolved (Fig. 2).

Method validation

Linearity. The correlation coefficients (r^2) for most of the 29 standards were higher than 0.99 (in the range of 0.5–125 or 1–250 μg/mL). Exceptions were thymine and adenosine which showed poor linear regression with lower concentration samples. The linearity was improved by excluding the low concentration data (Table 2). Similarly, the correlation coefficients (r^2) for most of the corresponding metabolites in liver tissue were higher than 0.98 (in the range of 0.02–0.25 g/mL); showing good linearity of the method (Table 2).

Limit of detection. The threshold of signal-to-noise (S/N) ratio of 3.0 is generally used to determine the limit of detection of the compound of interest in mass spectral analysis. However, due to a large number of reference compounds, the limit of detection in our study was determined by the minimum concentration of these compounds detected, shown as pg on column (see Table 2), with an S/N value provided, usually greater than 3.

Precision, reproducibility, stability, and recovery. The results demonstrate that the instrument has good precision. Approximately 40% of the compounds had RSD values below 5%, the rest were less than 8%. For most of the compounds investigated, the RSD values of reproducibility and stability were below 10% and 15%, respectively, demonstrating the reliability of the whole analytical method (see Table 3). The organic acids and fatty acids showed higher RSD values than other chemical classes investigated both for reproducibility and stability. As shown in Table 4, mean recovery of typical metabolites ranged from 63.2% to 99.0% with almost all of the RSD of recovery lower than 10%, demonstrating the reliability of the extraction method.

Table 3: Precision, reproducibility, and stability.

Compounds	**Precision RSD (%): standards (*n* = 6)**	**Reproducibility RSD (%): tissue samples (*n* = 6)**	**Stability RSD (%): tissue samples (*n* = 8)**
Amino acids			
Tyrosine	3.4	4.8	8.1
Tryptophan	6.0	6.7	9.0
Glycine	6.5	9.7	11.2
Proline	5.6	10.0	15.0
Aspartic acid	6.2	8.3	8.5
Methionine	5.0	9.3	9.2
Valine	5.9	9.1	8.5
Alanine	5.3	9.4	14.5
Serine	6.5	8.0	8.6
Isoleucine	4.9	9.4	11.0
Histidine	2.8	12.3	14.0
Threonine	6.1	8.4	9.6
Asparagine	2.9	9.6	13.6
Ornithine	2.9	6.0	6.9
Lysine	3.3	9.9	5.9
4-Aminobutyric acid	4.2	9.8	4.9
Organic acids			
Citric acid	4.1	10.0	8.6
Succinic acid	6.1	13.6	12.7
α-Ketoglutaric acid	3.7	10.1	11.5
Carbohydrates			
Fructose	7.3	8.1	8.9
Arabitol	7.4	7.1	8.7
Gluconic acid	3.6	7.5	7.7
Fatty acids			
Tetradecanoic acid	3.6	10.1	14.7

Hexadecanoic acid	3.8	15.9	15.2
Oleic acid	3.5	12.0	18.2
Octadecanoic acid	6.8	9.6	8.7
Nucleotides			
Thymine	8.0	9.9	9.8
Adenosine	6.7	9.5	13.5
Uridine	7.9	5.0	9.1

Table 4: Recovery of typical metabolites.

Compounds	Mean recovery (%)[a]	RSD (%)[a]
Tyrosine	92.9	4.7
Tryptophan	80.5	6.6
Proline	88.4	8.9
Methionine	81.1	4.1
Valine	87.4	7.2
Serine	97.2	8.5
Isoleucine	93.4	5.9
Histidine	81.2	2.4
Asparagine	85.0	7.7
Ornithine	99.0	4.5
Lysine	83.1	9.2
Citric acid	66.0	6.0
Arabitol	74.7	4.3
Gluconic acid	92.4	1.7
Adenosine	63.2	12.5

[a]Mean recovery and RSD were obtained by 9 determinations (3 parallel samples at 3 different concentrations) with the internal standard adjustment.

Application

Assays of serum and hepatic components and enzymes. Serum alanine aminotransferase (ALT), aspartate aminotransferase (AST), total bilirubin (TBIL), and cholesterol (CHOL) were measured with an auto-biochemistry detector in Shanghai Sixth Hospital (Shanghai, China). Hepatic malondialdehyde (MDA) and superoxide dismutase (SOD) were determined using commercial kits purchased from the Jiancheng Institute of Biotechnology (Nanjing, China). All values in Table 5 were presented as mean ± SD. For a single comparison between the two groups, *t*-test determined the significance of group differences. A level of $P < 0.05$ was taken as statistically significant and a level of $P < 0.01$ as most significant. As shown in Table 5, serum ALT and AST activities in rats intoxicated with CCl_4 dramatically increased 24 h after the second injection. A significant increase in serum TBIL and hepatic MDA, and a significant decrease in serum CHOL and hepatic SOD in the model group were also observed. All the biochemical results indicated that CCl_4 had already caused acute liver injury in the model rats.

Table 5: Serum and hepatic biochemical analysis.

Compounds	Control (n = 10)	Model (n = 10)
ALT (U/L)	44 ± 8	901 ± 158[a]
AST (U/L)	185 ± 35	1022 ± 173[a]
TBIL (μmol/L)	2.3 ± 0.5	4.4 ± 1.4[b]
CHOL (mmol/L)	1.3 ± 0.2	1.1 ± 0.3[b]
MDA (nmol/mgprot)	5.8 ± 1.7	15.1 ± 6.9[a]
SOD (U/mgprot)	182 ± 45	124 ± 55[b]

[a]$P < 0.01$.
[b]$P < 0.05$.

Liver tissue metabonomic study. Liver tissues obtained from CCl_4-induced liver injury model rats (n = 10) and control rats (n = 10) were treated with our established two-step extraction method and derivatization procedure. Fig. 3a shows obvious differences between the model and control groups in the typical GC/TOFMS total ion current (TIC) chromatograms.

Figure 3: (a) Typical GC/TOFMS total ion current (TIC) chromatograms of liver tissue samples from a model rat (the upper) and a control rat (the bottom). The keys are provided in Table 6 and (b) OPLS-DA scores plot of GC/TOFMS data from liver tissue samples of models (triangle) and controls (square).

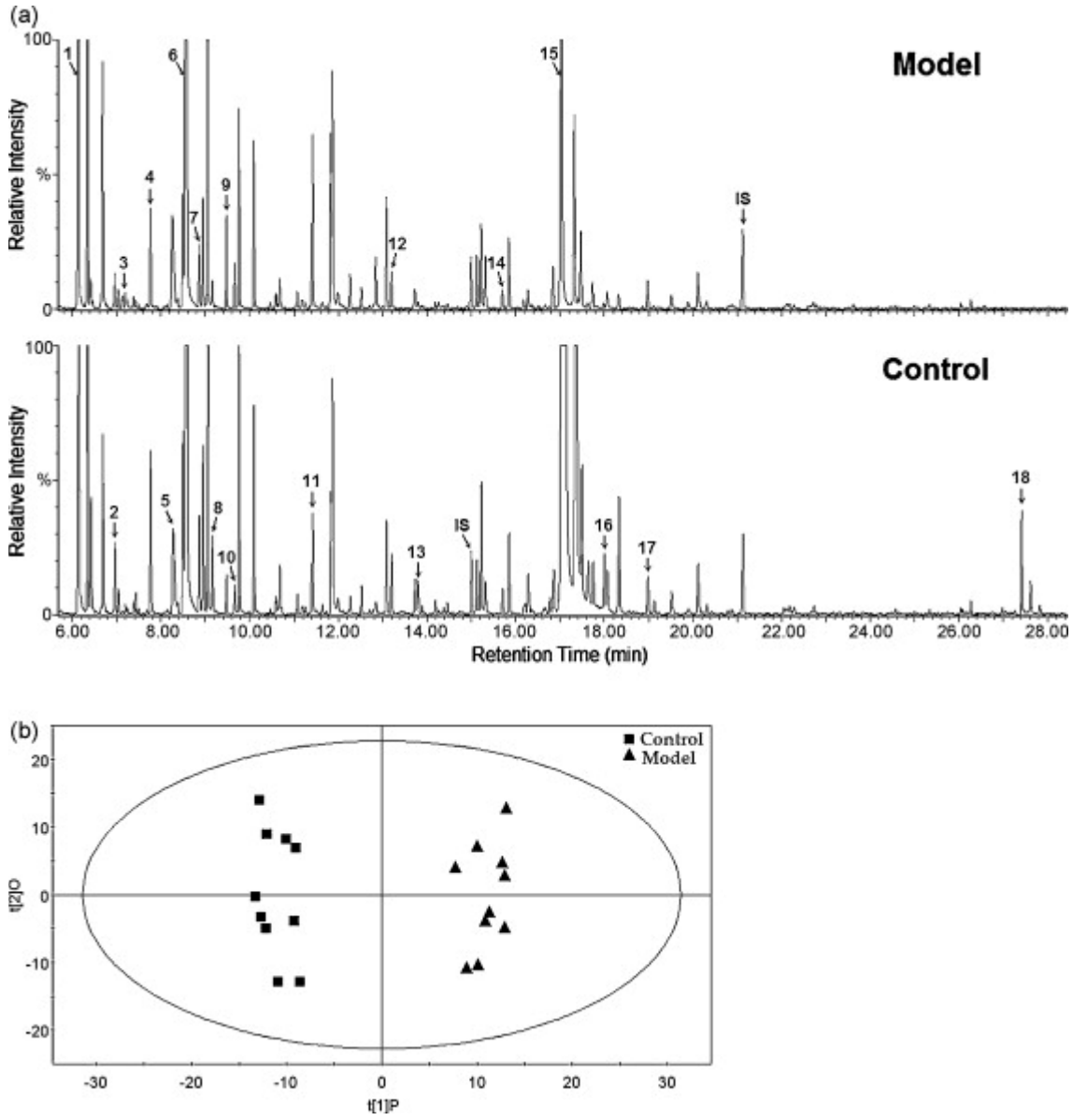

To explore metabolic differences between the model rats and the control group, the obtained GC/TOFMS data were analyzed using multivariate statistics. The initial unsupervised PCA model illustrates the natural but clear separation between model and control samples (figure not shown). Additionally, an OPLS-DA model (R^2Y = 0.976, Q^2Y = 0.911; Fig. 3b) was constructed to identify the differential metabolites contributing to the separation of these two groups. The percentages of variance explained by the first and second components in the model are 23.6% and 16.0%, respectively. Variable importance in the projection (VIP) ranks the overall contribution of each variable (peak intensity) to the OPLS-DA model—variables with VIP > 1 were selected as differential signals [9] and [12]. Accordingly, we identified a total of 18 differential metabolites in our study using NIST library, and 11 of them were confirmed by standard compounds (Table 6).

Table 6: A list of identified differential metabolites derived from multidimensional analysis.

	Metabolites	RT (min)	VIP[a]	Trend[b]
1	Alanine[c]	6.14	1.38	↓
2	beta-Hydroxybutyric acid	6.96	1.08	↓
3	Phosphoric acid	7.19	1.24	↑
4	Valine[c]	7.76	1.08	↓
5	Urea	8.21	1.27	↑
6	Glycerol	8.58	1.49	↓
7	Isoleucine[c]	8.86	1.13	↓
8	Succinic acid[c]	9.16	1.69	↓
9	Uracil	9.47	1.81	↑
10	Fumaric acid[c]	9.66	1.27	↑
11	Malic acid[c]	11.42	1.27	↑
12	Phenylalanine[c]	13.20	1.31	↓
13	Arabitol[c]	13.80	1.73	↓
14	Hypoxanthine[c]	15.70	1.19	↓
15	Glucose	17.06	1.71	↓
16	Gluconic acid[c]	18.07	1.25	↓
17	Xanthine[c]	18.98	1.30	↓
18	Maltose	27.41	1.71	↓

[a]Variable importance in the projection (VIP) indicates the relative influence of each metabolite to the grouping; metabolites with higher VIP values are more influential.
[b]↑ indicates that the metabolite is increased in the model compared to the control; ↓ indicates that the metabolite is decreased in the model compared to the control.
[c]Confirmed by standard compounds in addition to NIST.

CCl_4 is widely used as a toxin to induce liver injury in rats. The toxicity induced by CCl_4 is recognized by free radicals, mainly trichloromethyl radical (.CCl_3) and its peroxyl radical (.$OOCCl_3$), which initiate the chain reaction of lipid peroxidation and cause subsequent cell damage [30,31]. Recently, Huang et al. [32] performed GC/MS-based metabolic profiling of plasma in CCl_4-induced mice and Lin et al. [33] introduced LC/MS for metabonomic analysis of urine from CCl_4-induced rats. In the current study, we conducted metabonomic profiling of rat liver tissue, the precise location of CCl_4-induced damage. Therefore, the differential metabolites derived from our liver-targeted metabonomic study may provide more direct biochemical information of the local acute phase response of hepatocytes after CCl_4 intoxication.

In our study, significant decreases in glucose, gluconic acid and maltose concentrations in the acute liver injury model group, as compared with control group, were observed. These may be the combined effects of both inhibited gluconeogenesis and glycolysis under oxidative stress caused by CCl_4[34]. The decreased levels of the amino acids detected in the model group are

consistent with the theory that CCl_4 intoxication leads to the inhibition of amino acid uptake and protein synthesis [30,35]. TCA cycle is also found disturbed as important intermediates succinic acid declines; malic acid and fumaric acid augment in the model group. Meanwhile, the increased levels of malic acid, fumaric acid and urea observed in the model group may reflect the up-regulated urea cycle after CCl_4 intoxication, which is also consistent with the decreases of many amino acids in the model. Moreover, significant increase in uracil and decreases in xanthine and hypoxanthine were also detected in the model group, which may indicate disturbances in nucleotide (pyrimidine and purine) metabolism in CCl_4-induced acute liver injury rats.

CONCLUSTION

In this study, we developed and optimized a two-step extraction method for GC/TOFMS-based tissue metabonomic study, using a solvent mixture of chloroform, methanol, and water (1:2:1, v/v/v) for the first step, followed by a second extraction with methanol alone. This method has been extensively tested and validated using 29 standard compounds from different chemical classes and healthy rat liver tissues, and practically applied to metabonomic analysis of liver tissue samples from a rat model of CCl_4-induced liver injury. Analytical variations due to the instrument and extraction method were insignificant compared to the biological variations associated with liver injury, proving the feasibility of this method in detecting perturbed metabolic networks in tissue metabonomic studies.

ACKNOWLEDGEMENTS

This work is funded by the National Basic Research Program of China (Project numbers 2007CB914700, 2007CB511905), the Ministry of Science and Technology of the People's Republic of China (Project number 2006BAI08B04-01) and Research Projects of the Shanghai Science and Technology Commission (Project Number 064307067, 06DZ05906).

REFERENCES

[1] J.C. Lindon, E. Holmes, J.K. Nicholson, Metabonomics techniques and applications to pharmaceutical research & development, Pharm. Res. 23 (2006) 1075–1088.

[2] J.K. Nicholson, J. Connelly, J.C. Lindon, E. Holmes, Metabonomics: a platform for studying drug toxicity and gene function, Nat. Rev. Drug Discov. 1 (2002) 153–161.

[3] Y. Qiu, M. Su, Y. Liu, M. Chen, J. Gu, J. Zhang, W. Jia, Application of ethyl chloroformate derivatization for gas chromatography–mass spectrometry based metabonomic profiling, Anal. Chim. Acta 583 (2007) 277–283.

[4] Y. Ni, M. Su, Y. Qiu, M. Chen, Y. Liu, A. Zhao, W. Jia, Metabolic profiling using combined GC–MS and LC–MS provides a systems understanding of aristolochic acid-induced nephrotoxicity in rat, FEBS Lett. 581 (2007) 707–711.

[5] T. Levandi, C. Leon, M. Kaljurand, V. Garcia-Canas, A. Cifuentes, Capillary electrophoresis time-of-flight mass spectrometry for comparative metabolomics of transgenic versus conventional maize, Anal. Chem. 80 (2008) 6329–6335.

[6] J. Trygg, E. Holmes, T. Lundstedt, Chemometrics in metabonomics, J. Proteome Res. 6 (2007) 469–479.

[7] Q. Shen, X. Li, Y. Qiu, M. Su, Y. Liu, H. Li, X. Wang, X. Zou, C. Yan, L. Yu, S. Li, C. Wan, L. He, W. Jia, Metabonomic and metallomic profiling in the amniotic fluid of malnourished pregnant rats, J. Proteome Res. 7 (2008) 2151–2157.

[8] C.L. Gavaghan, I.D. Wilson, J.K. Nicholson, Physiological variation in metabolic phenotyping and functional genomic studies: use of orthogonal signal correction and PLS-DA, FEBS Lett. 530 (2002) 191–196.
[9] S. Wiklund, E. Johansson, L. Sjostrom, E.J. Mellerowicz, U. Edlund, J.P. Shockcor, J. Gottfries, T. Moritz, J. Trygg, Visualization of GC/TOF-MS-based metabolomics data for identification of biochemically interesting compounds using OPLS class models, Anal. Chem. 80 (2008) 115–122.
[10] K.E. Price, C.E. Lunte, C.K. Larive, Development of tissue-targeted metabonomics. Part 1. Analytical considerations, J. Pharm. Biomed. Anal. 46 (2008) 737–747.
[11] M.R. Viant, B.G. Lyeth, M.G. Miller, R.F. Berman, An NMR metabolomic investigation of early metabolic disturbances following traumatic brain injury in a mammalian model, NMR Biomed. 18 (2005) 507–516.
[12] Y. Ni, M. Su, J. Lin, X. Wang, Y. Qiu, A. Zhao, T. Chen, W. Jia, Metabolic profiling reveals disorder of amino acid metabolism in four brain regions from a rat model of chronic unpredictable mild stress, FEBS Lett. 582 (2008) 2627–2636.
[13] J. Lin, M. Su, X. Wang, Y. Qiu, H. Li, J. Hao, H. Yang, M. Zhou, C. Yan, W. Jia, Multiparametric analysis of amino acids and organic acids in rat brain tissues using GC/MS, J. Sep. Sci. 31 (2008) 2831–2838.
[14] N.J. Serkova, M. Jackman, J.L. Brown, T. Liu, R. Hirose, J.P. Roberts, J.J. Maher, C.U. Niemann, Metabolic profiling of livers and blood from obese Zucker rats, J. Hepatol. 44 (2006) 956–962.
[15] B.U. Bradford, T.M. O'Connell, J. Han, O. Kosyk, S. Shymonyak, P.K. Ross, J. Winnike, H. Kono, I. Rusyn, Metabolomic profiling of a modified alcohol liquid diet model for liver injury in the mouse uncovers new markers of disease, Toxicol. Appl. Pharmacol. 232 (2008) 236–243.
[16] N.J. Waters, E. Holmes, C.J. Waterfield, R.D. Farrant, J.K. Nicholson, NMR and pattern recognition studies on liver extracts and intact livers from rats treated with alpha-naphthylisothiocyanate, Biochem. Pharmacol. 64 (2002) 67–77.
[17] M. Chen, L. Zhao, W. Jia, Metabonomic study on the biochemical profiles of a hydrocortisone-induced animal model, J. Proteome Res. 4 (2005) 2391–2396.
[18] J.L. Griffin, L.A. Walker, S. Garrod, E. Holmes, R.F. Shore, J.K. Nicholson, NMR spectroscopy based metabonomic studies on the comparative biochemistry of the kidney and urine of the bank vole (Clethrionomys glareolus), wood mouse (Apodemus sylvaticus), white toothed shrew (Crocidura suaveolens) and the laboratory rat, Comp. Biochem. Physiol. B: Biochem. Mol. Biol. 127 (2000) 357–367.
[19] S.D. Huhn, C.M. Szabo, J.H. Gass, A.E. Manzi, Metabolic profiling of normal and hypertensive rat kidney tissues by hrMAS-NMR spectroscopy, Anal. Bioanal. Chem. 378 (2004) 1511–1519.
[20] O. Beckonert, H.C. Keun, T.M. Ebbels, J. Bundy, E. Holmes, J.C. Lindon, J.K. Nicholson, Metabolic profiling, metabolomic and metabonomic procedures for NMR spectroscopy of urine, plasma, serum and tissue extracts, Nat. Protoc. 2 (2007) 2692–2703.
[21] W. Weckwerth, K. Wenzel, O. Fiehn, Process for the integrated extraction, identification and quantification of metabolites, proteins and RNA to reveal their co-regulation in biochemical networks, Proteomics 4 (2004) 78–83.

[22] J.E. Le Belle, N.G. Harris, S.R. Williams, K.K. Bhakoo, A comparison of cell and tissue extraction techniques using high-resolution 1HNMRspectroscopy,NMR Biomed. 15 (2002) 37–44.
[23] R.K. Tyagi, A. Azrad, H. Degani, Y. Salomon, Simultaneous extraction of cellular lipids and water-soluble metabolites: evaluation by NMR spectroscopy, Magn. Reson. Med. 35 (1996) 194–200.
[24] H. Wu, A.D. Southam, A. Hines, M.R. Viant, High-throughput tissue extraction protocol for NMR- and MS-based metabolomics, Anal. Biochem. 372 (2008) 204–212.
[25] A. Jiye, J. Trygg, J. Gullberg, A.I. Johansson, P. Jonsson, H. Antti, S.L. Marklund, T. Moritz, Extraction andGC/MSanalysis of thehumanblood plasmametabolome, Anal. Chem. 77 (2005) 8086–8094.
[26] P. Jonsson, J. Gullberg, A. Nordstrom, M. Kusano, M. Kowalczyk, M. Sjostrom, T. Moritz, A strategy for identifying differences in large series of metabolomics samples analyzed by GC/MS, Anal. Chem. 76 (2004) 1738–1745.
[27] P. Jonsson, A.I. Johansson, J. Gullberg, J. Trygg, A. Jiye, B. Grung, S. Marklund, M. Sjostrom, H. Antti, T. Moritz, High-throughput data analysis for detecting and identifying differences between samples in GC/MS-based metabolomics analyses, Anal. Chem. 77 (2005) 5635–5642.
[28] S. Wold, M. Sjostrom, L. Eriksson, PLS-regression: a basic tool of chemometrics, Chemometr. Intell. Lab. Syst. 58 (2001) 109–130.
[29] H. Stenlund, A. Gorzsas, P. Persson, B. Sundberg, J. Trygg, Orthogonal projections to latent structures discriminant analysis modeling on in situ FT-IR spectral imaging of liver tissue for identifying sources of variability, Anal. Chem. 80 (2008) 6898–6906.
[30] L.W. Weber, M. Boll, A. Stampfl, Hepatotoxicity and mechanism of action of haloalkanes: carbon tetrachloride as a toxicological model, Crit. Rev. Toxicol. 33 (2003) 105–136.
[31] R.O. Recknagel, E.A. Glende Jr., J.A. Dolak, R.L. Waller, Mechanisms of carbon tetrachloride toxicity, Pharmacol. Ther. 43 (1989) 139–154.
[32] X. Huang, L. Shao, Y. Gong, Y. Mao, C. Liu, H. Qu, Y. Cheng, A metabonomic characterization of CCl4-induced acute liver failure using partial least square regression based on the GC/MS metabolic profiles of plasma in mice, J. Chromatogr. B: Anal. Technol. Biomed. Life Sci. 870 (2008) 178–185.
[33] Y. Lin, D. Si, Z. Zhang, C. Liu, An integrated metabonomic method for profiling of metabolic changes in carbon tetrachloride induced rat urine, Toxicology 256 (2009) 191–200.
[34] K.K. Singh, Oxidative Stress, Disease and Cancer, Imperial College Press, London, 2006.
[35] E.A. Smuckler, E.P. Benditt, Studies on carbon tetrachloride intoxication. 3. A subcellular defect in protein synthesis, Biochemistry 4 (1965) 671–679.